Thin Solid Films xxx (2012) xxx–xxx

Contents lists available at SciVerse ScienceDirect

Thin Solid Films

journal homepage: www.elsevier.com/locate/tsf

Monitoring of incorporation of magnetic ions into II–VI semiconductor nanocrystals by optical and magneto-optical spectroscopy

A.I. Savchuk *, I.D. Stolyarchuk, T.A. Savchuk, M.M. Smolinsky, O.A. Shporta, L.M. Shynkura

Department of Physics of Semiconductors and Nanostructures, Chernivtsi National University, 2 Kotsyubynsky Street, 58012 Chernivtsi, Ukraine

ARTICLE INFO

Available online xxxx

Keywords:
Diluted magnetic semiconductors (DMSs)
CdS:Mn
Nanocrystals
Growth monitoring
Optical density
Photoluminescence
Faraday rotation

ABSTRACT

Colloidal CdS:Mn semiconductor nanocrystals are synthesized by co-precipitation method using different concentrations of the $CdCl_2$, $MnCl_2$, Na_2S precursors and the capping agent. UV–vis absorption, photoluminescence and Faraday rotation spectra were combined for monitoring the formation of nanoparticles and incorporation of Mn magnetic ions into CdS nanoparticles. Through step by step observation of the absorption edge structure in the absorption spectrum of colloidal suspension the CdS:Mn nanocrystal growth was monitored, whereas dopant incorporation was controlled through changes in photoluminescence and Faraday rotation spectra. Faraday rotation spectra in CdS:Mn nanocrystals demonstrate peculiarities, which are associated with s, p–d exchange interaction between magnetic ions and band carriers in these nanostructures.

1. Introduction

In the past two decades, colloidal semiconductor nanocrystals (or quantum dots) have attracted much attention because of research interests and industrial applications such as light emitting diodes [1], lasers [2], solar cells [3] and biomedical labeling [4,5].

There is particular interest to transition metal-doped II–VI semiconductor nanocrystals, which have been widely studied from point of view affecting electronic, magnetic and optical properties and giving additional functionalities. Since these impurities can be paramagnetic, they introduce a localized spin into the nanoparticle, and form the so called diluted magnetic semiconductors (DMSs). DMSs are very promising materials for spintronic devices operating at room temperature.

However, magnetic impurity doping in II–VI colloidal semiconductor nanocrystals still remains a challenge [6–8]. Introducing magnetic ions inside the semiconductor host lattice is always controversial due to the incompatibility of dopants with the host lattice and difficulty of the "surface absorption" of impurities on the nanocrystal surface. The extent of efficient doping definitely depends on the synthesis method employed, where a control is needed to ascertain the concentration and location of dopants in the nanocrystal ensemble. Doping is only possible when lattice incorporation and diffusion of the dopant ions overcome the "self-purification" process. It was found [7] that much easier to dope nanocrystals with a zinc-blende crystal structure (CdS, ZnS, ZnSe), particularly if they contain a large proportion of (001) facets. In contrast, nanocrystals with a wurtzite structure (CdSe) are much more difficult to dope with Mn.

In the present study, we have synthesized CdS nanoparticles doped with Mn by a chemical precipitation technique using different concentrations of the Cd, Mn, S precursors and the capping agent. During the process of co-precipitation reaction of the precursors such characteristics as optical absorption, photoluminescence and magneto-optical Faraday rotation spectra were measured. Through step by step observation of the absorption edge structure in the absorption spectrum of colloidal suspension the CdS:Mn nanocrystal growth was monitored, whereas dopant incorporation was controlled through changes in photoluminescence and Faraday rotation spectra.

2. Experimental details

The synthesis techniques used to prepare the CdS:Mn nanocrystals were developed on the base of analysis of previously elaborated approaches. The growth of nanocrystals depends on a number of parameters, such as the surface energy of the nanocrystals, the concentration of free species in a solution, and the nanocrystal size, and thus the nanocrystal growth can be controlled by considering these parameters.

Nanocrystals of CdS:Mn were synthesized in aqueous medium by a chemical precipitation technique using cadmium chloride $CdCl_2$, manganese chloride $MnCl_2$ and sodium sulfide Na_2S in the presence of mercaptoethanol or polyvinylalcohol (PVA) as the capping agent. For Mn doping, an aqueous solution of $MnCl_2$ was added directly to the solution of $CdCl_2$ in the ratio 97:3. For all the samples the weight percentage of Mn was kept fixed (3%). Since all initial reaction conditions require cadmium to be in an excess of 2 to 1 sulfur, the latter is a limiting reagent and is completely consumed as particles mature. The addition of more sulfur allows the particles to grow to larger sizes.

Transmission electron microscopy (TEM) was used to confirm the nanocrystallinity of the grown samples, estimate shape and determine

* Corresponding author. Tel.: +380 372 584755; fax: +380 372 544897.
E-mail address: a.savchuk@chnu.edu.ua (A.I. Savchuk).

0040-6090/$ – see front matter © 2012 Elsevier B.V. All rights reserved.
http://dx.doi.org/10.1016/j.tsf.2012.10.127

the average size of nanoparticles. A TEM instrument which modified the UEMV-100 V microscopy that provides maximum resolution of 0.7 nm has been used.

In situ absorption spectra between 250 and 650 nm were measured using a grating monochromator, photodetector system and registered computer system as shown in Fig. 1. The monochromatic beam was focused into a quartz tube with an optical path length of 18 mm. In similar, in situ manner were registered also photoluminescence spectra. The samples were excited using a 325 nm He–Cd laser with an excitation intensity value of 10 mW.

Ex situ Faraday rotation measurements were carried out using a home-designed setup. As the rotation angle is proportional to the distance traveled by the light experimental measurements of this effect in low-dimensional semiconductor structures is a problematic task [9,10]. A iodine–halogen lamp is used as the radiation source and a grating monochromator with high resolution is used to yield monochromatic light in range of (200–2200) nm. After passing through a focusing lens and a polarizer (Roshon prism), monochromatic light becomes a linear polarized and then propagates through the studied sample placed in the electromagnet with magnetic field up to maximum induction 5 T. Behind the electromagnet the analyzer (Wollaston prism) splits the beam into two, which then pass through chopper. In such a manner these two beams were modulated by a phase shift of 180°. In the absence of magnetic field a balance was achieved by equalizing the intensities of the two light beams, and when the electromagnet was switch on the resultant unbalanced signal can be recorded by using photodetector system, which includes photomultiplier tube, lock-in amplifier and personal computer. The described setup allows to register the rotation angle of 10^{-4} rad.

3. Results and discussion

TEM image of typical colloidal CdS:Mn nanoparticles is shown in Fig. 2. For this kind of microscopic analysis a drop of colloidal suspension is placing on special carbon-coated copper grid. As can be seen the shape of the nanoparticles is close to spherical and the average diameter of the nanoparticles is found to be approximately 25 nm.

To illustrate the influence of precursor amount on the growth kinetics, nanoparticle size and size distribution the optical absorption and photoluminescence spectra were recorded in situ during the growth process.

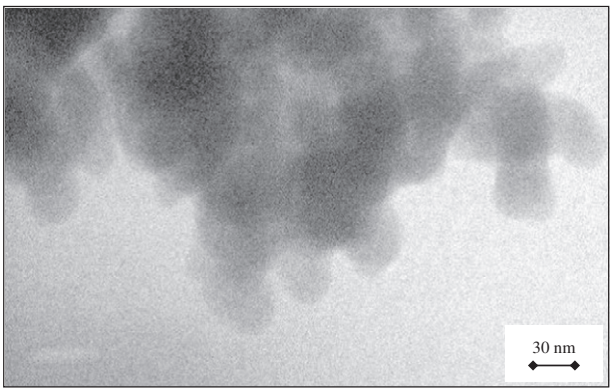

Fig. 2. TEM image of a typical sample of colloidal CdS:Mn nanocrystals.

Fig. 3 shows optical density as a function of photon energy for seven solution samples contained in the same quartz cuvette with inner thickness of 18 mm which corresponds to different amounts of precursors inside of the cuvette. Curve 1 corresponds to the sample with aqueous solution of mercaptoethanol without precursors. Curve 2 corresponds to minimal amounts of precursors (10^{-3} mol/l of $CdCl_2$ and Na_2S), so one can see beginning stage of nanoparticle growth process. The energy position of exciton band is indicated by arrows in Fig. 3. The observed broadening of the exciton structure can be attributed to both influence of dopant and effect of nanoparticle size distribution for the grown colloidal CdS:Mn nanoparticles. Further adding of precursors to the solution results in increase of optical density and shift of appropriate curves (3–7). However, exciton structure in these cases is slightly shifted to lower photon energy. Obviously, this is evidence of nearly constant average size of CdS:Mn nanoparticles, although their density in solution is increased. For large amounts of precursors (see curves 6, 7) optical absorption is much higher and range of photon energy which could be covered in experiments is restricted from the side of higher photon energy. In order to observe exciton band for these samples one should use another quartz container with smaller thickness. Therefore, to monitor growth process correctly and fully one should use a set of containers with different thicknesses.

Similar results on monitoring growth process were obtained from in situ measurements of photoluminescence spectra (Fig. 4). In the

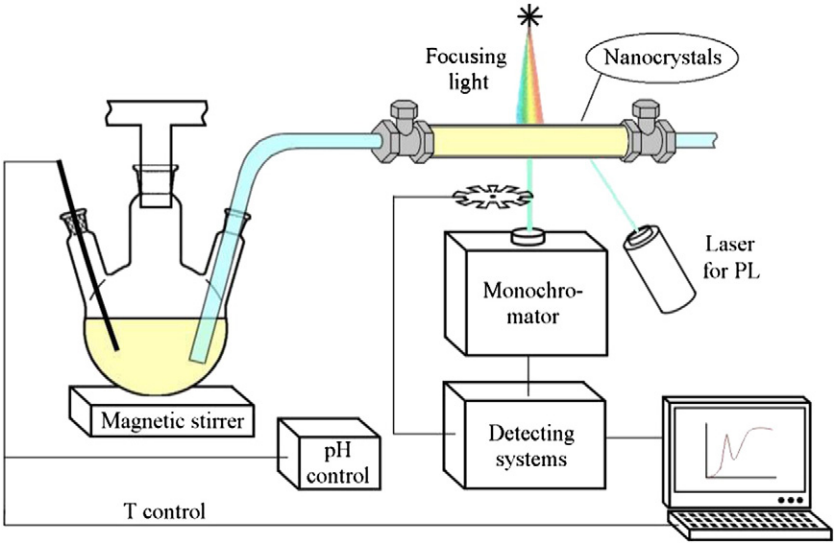

Fig. 1. Experimental setup for in situ measurements of optical absorption and photoluminescence spectra of colloidal semiconductor nanocrystals.

Please cite this article as: A.I. Savchuk, et al., Thin Solid Films (2012), http://dx.doi.org/10.1016/j.tsf.2012.10.127

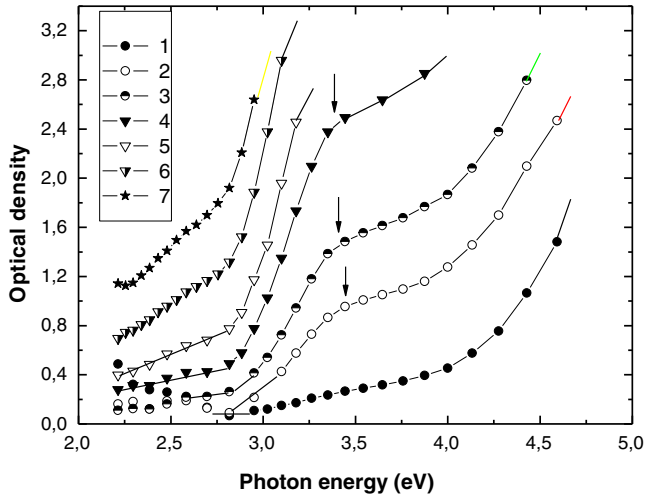

Fig. 3. Spectral dependence of optical density measured during the synthesis of CdS:Mn nanoparticles in mercaptoethanol solution.

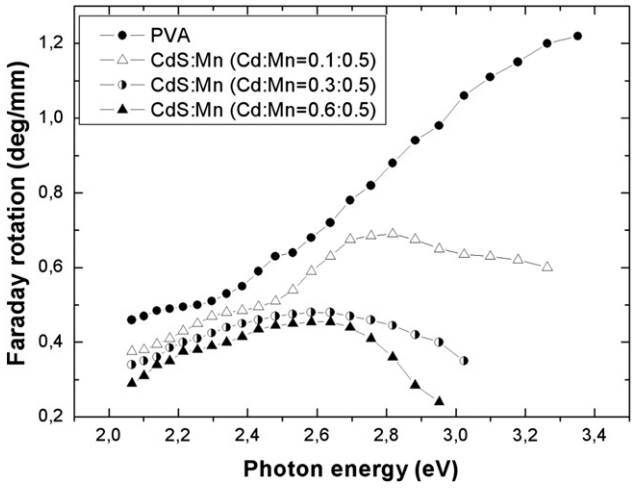

Fig. 5. Faraday rotation as a function of photon energy for colloidal CdS:Mn nanocrystals in aqueous PVA solution. The curves from up to down correspond to PVA solution only and to different Cd:Mn ratios of molar masses.

photoluminescence spectrum of CdS:Mn nanocrystals we have observed two emission bands. The emission band at 530 nm is due to radiative recombination of electrons and holes via the defect states in the nanoparticles [11]. The second emission band at 578 nm is due to $^4T_1 \rightarrow {}^6A_1$ transition of Mn^{2+} ions [12]. Namely this emission band can be used to monitor the incorporation of magnetic ions into the nanoparticles.

In order to elucidate the influence of $CdCl_2$, $MnCl_2$ and Na_2S precursor amount on the growth kinetics the Faraday rotation spectra of CdS:Mn nanocrystals have been recorded ex situ during the growth process in PVA solution. These measurements were performed in magnetic field with magnetic induction of 1 T. In Fig. 5 the upper curve corresponds to the sample with an aqueous solution of PVA without the precursors. Next three curves in up to down direction correspond to different Cd:Mn ratios of molar masses with the increased amounts of $CdCl_2$, $MnCl_2$ and Na_2S precursors. The decrease of the Faraday rotation is clearly observed from these data. Such a decrease without doubt is associated with the increase of content of semiconductor phase into solution and the presence of Mn impurity inside the CdS:Mn nanoparticles. It is well known that for DMS materials, the large exchange interaction between the band states of electrons (holes) and the localized d electrons of magnetic ions leads to strong enhancement of the Faraday rotation [13–15]. In the studied DMS nanocrystals a competition between diamagnetic and paramagnetic states should be exhibited as well. In fact, the observed decrease of the Faraday rotation and changes in its spectral dependence are associated with a positive and a negative part due to pure Zeeman and s, p–d exchange interaction contribution, respectively. According to the microscopic model of the Faraday rotation in bulk DMS [16,17] the Verdet constant as a function of photon energy $h\nu$ can be expressed as

$$V(h\nu) = Z\,f(h\nu) + CYg(h\nu) \quad (1)$$

where Z, C, Y are fitting parameters. The $f(h\nu)$ function has a positive sign, whereas $g(h\nu)$ function is negative. As a result, competition between these two contributions with opposite signs leads to the observed decrease of the Faraday rotation in the CdS:Mn nanocrystals shown in Fig. 5.

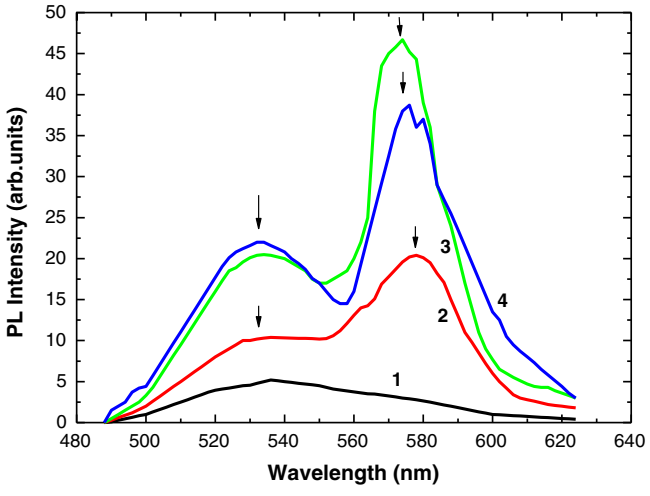

Fig. 4. Photoluminescence spectra measured during the synthesis of CdS:Mn in mercaptoethanol solution.

4. Conclusions

In conclusion, chemical synthesis of CdS:Mn nanocrystals was monitored by optical and magneto-optical spectroscopy. The absorption spectra showed a red shift when concentration of reagents is increased. The photoluminescence spectra of CdS:Mn nanocrystals exhibit two emission bands which are attributed to radiative recombination via defect states and to $^4T_1 \rightarrow {}^6A_1$ transitions of Mn^{2+} ions. The resulting Faraday rotation for CdS:Mn nanoparticles has negative sign which is attributed to contribution of s, p–d exchange interaction in zero-dimensional structures on the base of (II–VI):Mn DMSs.

Acknowledgments

This work has been supported in part by grant (No 12-800) from the Ministry of Education, Science, Youth and Sports of Ukraine.

References

[1] V.L. Colvin, M.C. Schlamp, A.P. Alivisatos, Nature 370 (1994) 354.
[2] V.I. Klimov, A.A. Mikhailovsky, S. Xu, A. Malko, J.A. Hollingsworth, C.A. Leatherdale, H.J. Eisler, M.G. Bawendi, Science 290 (2000) 314.
[3] N.C. Greenham, X.G. Peng, A.D. Alivisatos, Phys. Rev. B 54 (1996) 17628.
[4] W.C.W. Chan, S.M. Nie, Science 281 (1998) 2016.
[5] A.I. Savchuk, M.M. Marchenko, T.A. Savchuk, S.A. Ivanchak, V.I. Fediv, I.S. Davydenko, D.I. Ostafiychuk, Sens. Lett. 8 (2010) 419.
[6] D.J. Norris, Al.L. Efros, S.C. Erwin, Science 319 (2008) 1776.
[7] S.C. Erwin, L. Zu, M.I. Haftel, Al.L. Efros, T.A. Kennedy, D.J. Norris, Nature 436 (2005) 91.

[8] S. Bhattacharyya, Y. Estrin, D.H. Rich, D. Ziboun, Y. Koltypin, A. Gedanken, J. Phys. Chem. C 114 (2010) 22002.
[9] M. -H. Kim, V. Kurz, G. Achas, C.T. Ellis, J. Cerne, J. Opt. Soc. Am. B 28 (2011) 199.
[10] I. Crassee, J. Levallois, A.L. Walter, M. Ostler, A. Bostwick, E. Rotenberg, T. Seyller, D. van der Marel, A.B. Kuzmenko, Nature Phys. 7 (2011) 48.
[11] S.K. Mishra, R.K. Srivastava, S.G. Prakash, R.S. Yadav, A.C. Panday, J. Alloys Compd. 513 (2012) 118.
[12] X. Ma, J. Song, Z. Yu, Thin Solid Films 519 (2011) 5043.
[13] A.V. Komarov, S.M. Ryabchenko, O.V. Terletskij, I.I. Zheru, R.D. Ivanchuk, Sov. Phys. JETP 46 (1977) 318.
[14] J.A. Gaj, R.R. Galazka, M. Nawrocki, Solid State Commun. 25 (1978) 193.
[15] P.I. Nikitin, A.I. Savchuk, Sov. Phys. Usp. 33 (1990) 974.
[16] C. Buss, S. Hugonnard-Bruyere, R. Frey, C. Flytzanis, Solid State Commun. 92 (1994) 929.
[17] S. Hugonnard-Bruyere, C. Buss, F. Vouilloz, R. Frey, C. Flytzanis, Phys. Rev. B 50 (1994) 2200.

Please cite this article as: A.I. Savchuk, et al., Thin Solid Films (2012), http://dx.doi.org/10.1016/j.tsf.2012.10.127